DRL Based Beam Management for Joint Sensing and Communications in HSR mmWave Wireless Networks

Li Yan[1], Xuming Fang[1], Saifei Li[1], Yi Li[2], Qing Xue[3]
[1]Southwest Jiaotong University, Chengdu 610031, China
[2]China Academy of Railway Sciences, Beijing, China
[3]Chongqing University of Posts and Telecommunications, Chongqing, China
Email: liyan@swjtu.edu.cn; xmfang@swjtu.edu.cn; lisaifei@swjtu.edu.cn; liyi_swjtu@foxmail.com; xueq@cqupt.edu.cn

2022 IEEE 95th Vehicular Technology Conference (VTC2022-Spring) | 978-1-6654-8243-1/22/$31.00 ©2022 IEEE | DOI: 10.1109/VTC2022-Spring54318.2022.9860354

***Abstract*—The abundant available spectrum resources have made millimeter wave (mmWave) communications the key feature of the fifth generation (5G) mobile communications, allowing ultra-high transmission capacity. Additionally, mmWave bands, already widely used in radar systems, show a great advantage in environment sensing. Based on these observations, to satisfy the ever-growing mobile service requirements, and meanwhile to improve the maintenance efficiency for high-speed railways (HSRs), in this paper, we present the joint sensing and communication HSR mmWave wireless network, where two mmWave beams are intelligently controlled to provide broadband communications and environment sensing, respectively. Moreover, to mitigate the inter-beam interference between communication beams and sensing beams, we propose a deep reinforcement learning (DRL) based beam management scheme, where the beamwidth and inter-beam spacing are adaptively adjusted according to dynamic wireless environments. Simulation results demonstrate that our proposed scheme can better balance the communication capacity and the sensing performance compared to conventional schemes with fixed beamwidth and inter-beam spacing.**

***Index Terms*—Joint sensing and communications; high-speed railway; mmWave communications; beam management; deep learning**

I. Introduction

In recent years, to support the evolution of railway industry towards the intelligent stage, high-speed railway (HSR) wireless networks are facing severe challenges in satisfying the ever-growing mobile service requirements[1]. Learning from the successful development experiences of the fifth generation (5G) mobile communications, broadband millimeter wave (mmWave) communications are brought in HSR to enhance the system capacity. From another point of view, owing to the broadband bandwidth enabling high distance resolution and the beam directionality enabling high angular resolution, mmWave bands are also employed for environment sensing in radar systems, which is also beneficial for HSR maintenance [2]. Being aware of the dual functions of mmWave bands on sensing and communications, the joint sensing and communications has been approved as one of the most important development directions in the future [3].

In mmWave communications, to overcome the severe propagation loss, directional beamforming plays an essential role in concentrating mmWave signal energy to prolong the propagation distance, which however poses a great threat to network coverage robustness. In our previous works [4], [5], to address this issue, we leveraged conventional frequency bands below 6GHz (abbreviated as sub-6GHz) to provide omnidirectional coverage and mmWave bands to augment capacity, forming the sub-6GHz and mmWave dual-band cooperation HSR wireless network architecture. In this paper, building on the sub-6GHz and mmWave integration, we further introduce the joint sensing and communication HSR mmWave wireless network, where two intelligently-controlled mmWave beams simultaneously provide broadband communications and environment sensing, and sub-6GHz bands carry related signaling to guarantee the transmission reliability. Different from our previous design in [6] where sensing and communications are implemented in a time division manner, in this study, during the movements of trains, mmWave sensing beams constantly detect the areas to be passed by trains, and collect the track inspection data for post processing, improving the HSR maintenance. Nevertheless, under this design, when there is no train, mmW-RRUs can also sweep sensing beams for obstacle detections and danger warning.

In the joint sensing and communication HSR mmWave wireless network, to pursue the integration gain between the two functions, sensing and communication beams are designed to share the same mmWave bandwidth and antenna arrays. Due to the sidelobe energy leakages, the inter-beam interferences will degrade the sensing and communication performance [7]. Intuitively, the beamwidth and inter-beam spacing of the sensing and communication beams, which directly determines the beam gain and the interference power, are two important parameters in balancing the sensing and communication performance. Consequently, we propose a deep reinforcement learning (DRL) based beam management scheme, where the beamwidth and inter-beam spacings are adaptively adjusted according to dynamic wireless environments, mitigating the inter-beam interferences. Finally, we present simulation results to demonstrate the effectiveness of our proposed scheme.

The rest of this paper is organized as follows. In section II, the joint sensing and communication HSR mmWave wireless network is illustrated. In section III, we introduce the DRL-based intelligent beam management scheme. In section IV, simulations and analysis are presented to demonstrate the effectiveness of the proposed scheme. Finally, in section V, we conclude this paper and prospect future study.

II. Network architecture

A. The joint sensing and communication HSR mmWave wireless network

Leveraging directional beamforming to overcome the severe propagation loss, mmWave communications have the native problem of low robust network coverage. In our previous works [4], [5], we designed the sub-6GHz and mmWave dual-band integrated HSR wireless network architecture, where sub-6GHz bands with omnidirectional coverage are employed to provide basic network coverage. As shown in Fig. 1, building on the integration of sub-6GHz and mmWave bands, the joint sensing and communication HSR mmWave wireless network architecture is presented. To facilitate the network management, we deploy the whole network based on the cloud radio access network (C-RAN) technology, where baseband processing resources gathered in the BBU pool are centrally controlled on demand, and the two types of remote radio units (RRUs), i.e., the low frequency RRUs (LF-RRUs) and the mmWave RRUs (mmW-RRUs), operate at sub-6GHz and mmWave bands, respectively. To guarantee the transmission reliability, joint sensing and communication related signaling, including beam management information, can be carried by LF-RRUs. To simultaneously implement sensing and communications during the movement of trains, mmW-RRUs point two mmWave beams at trains for communications and at the target areas for sensing, respectively. To reduce hardware costs, the sensing and communication beams share the same antenna array in our design, but are mutually orthogonal in the spatial domain [8]. To discover track faults during the traveling of trains, the target sensing areas in our study are defined as the areas in front of trains that they will pass through soon. On trains, we apply a two-hop access structure, consisting of an access point (AP) inside trains to collect service data and an mobile relay (MR) outside trains to forward service data to the ground. The MR is equipped with sub-6GHz and mmWave antennas to access the dual bands. Our study focuses on the communication link between roadside RRUs and MRs.

To enhance the utilization of scarce frequency resources, in our design, the sensing and communication beams share the same mmWave bandwidth, which however leads to the inter-beam interference problem challenging the joint sensing and communication performance. To mitigate inter-beam interference, the two beams should maintain a suitable spacing, namely inter-beam spacing denoted as $\Delta\phi$ in Fig. 1. The larger the inter-beam spacing, the lower the inter-beam interference. Nevertheless, to obtain the track inspection data with trains passing through, the sensing areas should be as close to trains as possible, and therefore the inter-beam space is practically limited. Additionally, beamwidth is another important parameter influencing the inter-beam interference power. For simplicity, we employ uniform linear arrays (ULAs) to generate sensing and communication beams, where the beamwidth is inversely proportional to the number of allocated antennas. To facilitate the analysis, in Fig. 1, the projection of mmW-RRUs on rails denotes the original point of the d-axis which depicts the traveling distance of trains. The target maximum sensing distance, the coverage radius, and the mmW-RRU to rail distance are denoted as S_{max}, R, and d_{min}, respectively. Besides, the initial access and beam tracking of mmWave communications in HSR, which have been sufficiently studied [9], [10], are assumed perfectly solved, leaving the study focus of this paper on the intelligent decisions of the beamwidth and inter-beam spacing for joint sensing and communications.

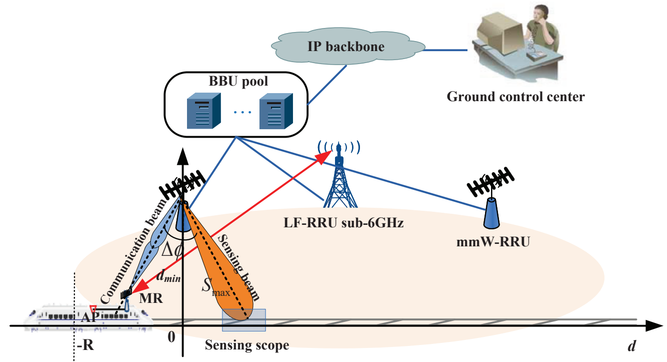

Fig. 1. The joint sensing and communications HSR mmWave wireless network.

B. The interference scenarios of joint sensing and communications

As sensing and communications are mutually orthogonal in the spatial domain, they use different waveforms in our design. Moreover, since we only care about the inter-beam interference power between sensing and communications instead of signal-level processing, the proposed scheme can be generalized to arbitrary radar systems. Without loss of generality, we assume the mmWave communications work in the time division duplexing (TDD) mode. To facilitate the understanding, in Fig. 2 we classify the interference scenarios based on the communication uplink and downlink directions. In the uplink interference scenario, the two mmW-RRU beams receive the uplink signals from trians and the sensing echo signals reflected from targets, respectively. With respect to the communication uplink receiving at mmW-RRUs, the simultaneously-radiated sensing signals from sensing beams cause self-interference. Considering that the self-interference cancellation (SIC) technology has achieved remarkable performance in reducing the self-interference[11], we assume the self-interference is perfectly cancelled to simplify the analysis. While for the receiving of sensing echo signals at mmW-RRUs, the uplink signals from trains cause interference, namely inter-beam interference. In the downlink interference scenario, the sensing signals radiated from mmW-RRUs interfere the receiving of communication downlink signals at trains, which is also the inter-beam interference. Simultaneously, the transmitted communication downlink signals interfere the receiving of sensing echo signals at mmW-RRUs, which however is the self-interference and can be cancelled through the SIC technology by mmW-RRUs. Since the communication receiving beams of trains point towards the direction of mmW-RRUs, we ignore the interference of sensing echo signals whose strength are already highly-faded, and only consider the inter-beam interference resulted from the radiated sensing signals of mmW-RRUs.

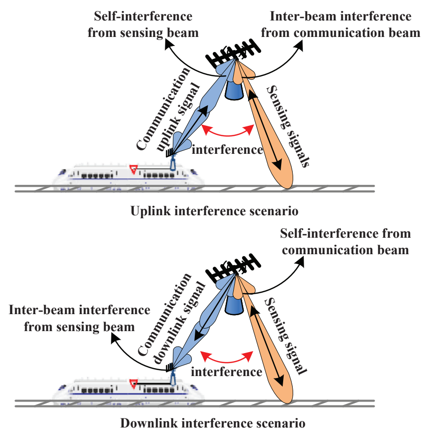

Fig. 2. The interference scenarios of joint sensing and communications.

III. The DRL based beam management scheme

In the joint sensing and communication HSR mmWave wireless network, two mmWave beams are simultaneously radiated for sensing and communications, respectively, involving the inter-beam interference issue. The inter-beam spacing and the beamwidth are two key parameters determining the level of inter-beam interference. Therefore, to guarantee the joint sensing and communication performance, in this section, we propose a DRL based beam management scheme as shown in Fig.3. Although in the current study we focus on the beam management under a single mmW-RRU, it is necessary to coordinate adjacent mmW-RRUs to facilitate the mobility management for communications and networked detections for sensing, which will be discussed in our future study. Consequently, by leveraging the central control capability of C-RAN, we implement the proposed algorithm in the BBU pool to realize the cooperation between mmW-RRUs. In the situations with normal mmWave communications, mmW-RRUs periodically report the sensing and communication states to the BBU pool through high-speed wired back-haul. If mmWave communication beams are interrupted due to beam management failures, the BBU pool can still control beams of trains through exchanging information on sub-6GHz bands via LF-RRUs. Based on the obtained states of sensing and communications, the BBU pool executes the proposed DRL-based beam management algorithm to decide the beamwidth and inter-beam spacing for the mmWave sensing and communication beams.

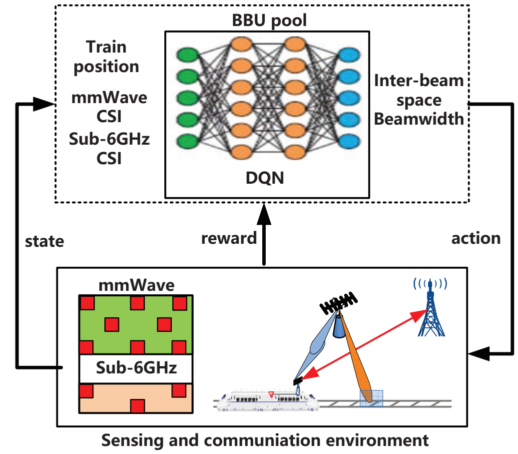

Fig. 3. The DQN-based beam management scheme for joint sensing and communications.

Signal to interference plus noise ratio (SINR) is the key metrics to evaluate both the sensing and communication performance. Next, we present the mathematical models of sensing SINR and communication SINR, and formulate our optimization problem. At receivers, the received signal power in decibel of mmWave communication beams is

$$P_{r,c}(d_c) = P_{t,c} + G\left(BW_c, \Delta\theta_{r,c}\right) + G\left(BW_c, \Delta\theta_{t,c}\right) - PL\left(d_c\right) \tag{1}$$

where $P_{t,c}$ is the transmit power of mmWave communication beams. d_c denotes the communication distance, which can be derived as $d_c = \sqrt{d^2 + {d_{\min}}^2}$ based on the geometric relationship in Fig. 1. $G\left(BW_c, \Delta\theta_{r,c}\right)$ and $G\left(BW_c, \Delta\theta_{t,c}\right)$ are the transmit and receiving beam gain, respectively, with [12]

$$G\left(BW, \Delta\theta\right) = 10\log_{10}\left(\frac{\pi}{BW} e^{-\eta\left(\frac{\Delta\theta}{BW}\right)^2}\right) \tag{2}$$

where the beamwidth BW is usually approximated as $BW = \frac{2\lambda}{n\Delta d}$ with λ, n, and Δd denoting the mmWave wavelength, the number of antennas, and the antenna spacing, respectively [13]. η is a constant parameter with value of $4\log_{10}2$. $\Delta\theta$ is the angle offset between the beam main lobe and the target pointing direction. To simplify the analysis, we assume the beam offsets due to beam misalignments follow the normal distribution, i.e., $\Delta\theta \sim N\left(0, \sigma_\theta^2\right)$, with zero mean and variance of σ_{θ_c}. In Eq. (1), the major propagation loss, i.e., the free spacing path loss, is usually modeled as $PL\left(d_c\right) = 10\log_{10}\left(\frac{\left(4\pi d_c\right)^2}{\lambda^2}\right) = 32.4 + 20\log_{10} f_c\left(GHz\right) + 20\log_{10} d_c\left(m\right)$, where f_c is the frequency center.

For simplicity, we assume the same configuration for the transmit and receiving antenna arrays radar systems, implying the same transmit gain and receiving gain. Then, the radar detection range equation has an expression of [14]

$$\begin{aligned} P_{r,s}\left(d_s\right) &= P_{t,s} + 2G\left(BW_s, \Delta\theta_s\right) + 10\log_{10}\left(\sigma_{RCS}\right) \\ &-10\log_{10}\left(\frac{\left(4\pi\right)^3}{\lambda^2}\right) - 40\log_{10}\left(d_s\right) \end{aligned} \tag{3}$$

where d_s, $P_{t,s}$, and σ_{RCS} are the sensing distance, transmit power of sensing beams, and the radar cross section (RCS) of targets, respectively. Similarly, the beam offsets of sensing with respect to targets are assumed to follow the normal distribution of $\Delta\theta_s \sim N\left(0, {\sigma_\theta}_s{}^2\right)$. Based on the geometric relationships in Fig. 1, the required maximum sensing distance S_{max} is

$$S_{\max} = \frac{d_{\min}}{\left|\cos\left(\Phi + \Delta\phi(d)\right)\right|} \tag{4}$$

where $\Phi = arctan\left(\frac{d}{d_{\min}}\right)$.

According to the inter-beam interference analysis in Section II.B, in the uplink interference scenario, the sensing receiving beams at mmW-RRUs are interfered by the communication uplink beams from trains, of which the inter-beam interference power can be modeled as

$$I_U = P_{t,train} + G\left(BW_c, \Delta\theta_{t,c}\right) + G\left(BW_s, \Delta\phi\right) - PL\left(d_c\right). \tag{5}$$

Then, at the maximum sensing distance S_{max}, the received minimum SINR of sensing can be expressed as

$$SINR_{min,s} = P_{r,s}\left(S_{max}\right) - 10\log_{10}\left(kTB\right) - NF - I_U \tag{6}$$

where k, T, B, and NF are the Boltzmann's constant, the system temperature, the bandwidth, and the receiver noise figure, respectively. Suppose the required SINR of radar systems is $SINR_{s,th}$ which is determined by the false alarm and detection probability as shown in [14], then the sensing SINR should satisfy $SINR_{min,s} > SINR_{s,th}$. Moreover, when the integration technology is used in receiving radar echo signals, the required SINR can be relaxed by $I(m)$ times, where $I(m)$ is the integration improvement factor and m is the integration number [14].

From the inter-beam interference analysis, the larger the inter-beam spacing, the lower the inter-beam interference. Nevertheless, to provide efficient track inspections with trains passing through, the sensing target areas should be as close to trains as possible. The sensing spacing distance between trains and the target detection areas can be calculated as

$$\Delta D_s(d) = \left|d_{\min}\tan\left(\Phi + \Delta\phi(d)\right) - d\right| \tag{7}$$

In the downlink interference scenario, for the communication receiving beams at trains, the inter-beam interference caused by the radiated sensing signals has the power of

$$I_D = P_{t,s} + G\left(BW_s, \Delta\theta_s\right) + G\left(BW_c, \Delta\phi\right) - PL(d_c). \tag{8}$$

Then, the achieved communication SINR and spectrum efficiency can be respectively calculated as

$$SINR_c(d_c) = P_{r,c}(d_c) - I_D(d_c) - N_0 \tag{9}$$

and

$$R_c = log_2(1 + SINR_c) \tag{10}$$

where N_0 is the noise power.

Based on the above derivations, we can find the received SINR of sensing and communication beams are highly-related with the inter-beam spacing and the beamwidth, which are therefore taken as two key control parameters to tune beams. As aforementioned, in our design, sensing and communication beams share the same antenna array. Suppose the total number of available antennas is n_t, sensing and communication beams use n_s and n_c antennas, respectively. Consequently, $BW_s = \frac{2\lambda}{n_s\Delta d}$ and $BW_c = \frac{2\lambda}{n_c\Delta d}$. In this paper, our optimization goal is to maximize the communication capacity under the constraint of basic sensing performance. Therefore, the problem can be modelled as

$$\begin{aligned} &\max_{\Delta\phi, BW_c, BW_s} \sum_{d=-R}^{R} \gamma_d R_c\left(d\right) - \sum_{d=-R}^{R} \Delta D_s\left(d\right) \\ &s.t. \quad 0 < \Delta\phi\left(d\right) < \Delta\phi_{\max} \qquad (a) \\ &\qquad SINR_{\min,s} > SINR_{s,th} \qquad (b) \\ &\qquad n_c + n_s \leq n_t \qquad (c) \end{aligned} \tag{11}$$

where the objective aims to maximize the communication capacity while minimizing the sensing spacing distance. Taking the beamwidth adjustment costs into account, a discount factor γ is defined, whose value is 1 when the beamwidth needs no adjustment, i.e., the beamwidth adopted at the current position is the same as that at the previous position, otherwise its value is smaller than 1 to discount the beamwidth adjustment costs. Constraint (a) restricts the inter-beam spacing, where $\Delta\phi_{\max}$ is the maximum allowed inter-beam spacing. The sensing SINR requirements are given in constraint (b). During the adjustment of beamwidth, the number of antennas used for sensing and communication beams should not exceed the total available antennas, which is stated in constraint (c). Obviously, this problem is a typical combinational optimization problem, and hard to solve.

In our optimization problem of Eq. (11), the beamwidth adjustment cost between two adjacent positions is considered, that is the current decision will influence the subsequent performance. Therefore, the decision of inter-beam spacing and beamwidth can be characterized as a Markov-decision process (MDP). The RL algorithms, which learn policy through trials and errors and make decisions intelligently according to environments, have been widely used to solve MDP problems. In this paper, we employ the model-free RL algorithm, i.e., the Q-learning algorithm, to decide inter-beam spacing and beamwidth, where the state, the action, and the reward, are respectively defined as follows. Moreover, in HSR, the movement patterns of trains along determined rails have strong regularity, leading to the strong regularity of wireless propagation environments in space and time. To a large degree, the off-line trained model can precisely match the on-line applications. Consequently, the computation complexity of the proposed scheme mainly happens in the off-line training phase, and in the on-line application phase the best action can be directly determined according to the current states without iterations.

State: the environment state in our problem includes the position of trains, the sub-6GHz SNR, the mmWave SINR, the communication beamwidth in the last state $t-1$, and the sensing beamwidth in the last state $t-1$, i.e., $\mathbf{s_t} = [d, SNR_{sub6}, SINR_c, SINR_{min,s}, BW_{c,t-1}, BW_{s,t-1}]$.

Action: the action consists of the inter-beam spacing and beamwidth of sensing and communication beams, i.e., $\mathbf{a_t} = [\Delta\phi, BW_c, BW_s]$.

Reward: based on the formulated optimization problem in Eq. (10), the step reward is defined as

$$\mathrm{Re_t} = \begin{cases} \gamma_d R_c(d) - \Delta D_s(d), SINR_{\min,s} > SINR_{s,th} \\ -\infty, otherwise \end{cases} \tag{12}$$

Nevertheless, with high-dimension states and actions, it is unreasonable to keep the look-up table of Q-values. The deep Q network (DQN), using deep neuron network (DNN) to approximate Q-values, can solve this problem, where the DNN parameter updates can be modelled as

$$\mathbf{v}_{t+1} = \mathbf{v}_t + \ell \Big(R_t(\mathbf{s}_t, \mathbf{a}_t) + \varsigma \max_{\mathbf{a}} Q(\mathbf{s}_{t+1}, \mathbf{a}_{t+1}, \mathbf{v}^-) \\ - Q(\mathbf{s}_t, \mathbf{a}_t, \mathbf{v}) \Big) \nabla Q(\mathbf{s}_t, \mathbf{a}_t, \mathbf{v}) \tag{13}$$

with ℓ, ς, and v representing the learning rate, the reward discount factor, and the Q-network parameter, respectively. Since the DQN algorithm has uniform implementation procedures, considering the space limitation, we just provide the main models of our problem, and more details about the DQN algorithm can be found in [15].

IV. Simulation Results and Analysis

Based on the theoretical models, in this section we conduct simulations and analyze the results to demonstrate the effectiveness of our proposed scheme. The parameter settings of simulations are listed in Table I. For fairness, we compare our scheme with the fixed inter-beam spacing and beamwidth schemes. In Fig. 4, the selected actions of the proposed scheme and the communication spectrum efficiency of different schemes are shown. From the results in Fig.4(b), we can find that owing to the optimization objective of maximizing the communication capacity, the proposed scheme with adaptive inter-beam spacing and beamwidth can achieve almost the same spectrum efficiency as the fixed inter-beam spacing and beamwidth schemes with antennas equally allocated for sensing and communication beams. Compared with sensing which aims at receiving echo signals, the receiving signals of communications only experience one trip propagation loss, thereby having higher tolerance to interference. Consequently, enlarging the inter-beam spacing has limited improvements on the communication capacity. While for the case with more antennas allocated for sensing beams, the communication capacity is heavily degraded due to the reduced beam gain.

TABLE I
THE MAIN SIMULATION PARAMETER SETTINGS [14].

Parameters	Values	Parameters	Values
d_{min}	20m	f_c	30GHz
$P_{t,c}$	23dBm	$P_{t,s}$	23dBm
σ_{RCS}	1m^2	NF	$10dB$
Boltzmann's constant	1.38×10^{-23}J/K	$I(m)$	10
Bandwidth	200MHz	n_t	100
$SINR_{s,th}$	6dB	Discount factor	0.2
ℓ	0.1	ς	0.9
Coverage	200m	$\Delta\phi_{\max}$	20^o

Areas	(-100m,-60m)	(-55m,-45m)	(-40m,45m)	(50m,75m)	(80m,100m)
Actions	n_c=60 n_s=40 $\Delta\phi$=9^o	n_c=50 n_s=50 $\Delta\phi$=10^o	n_c=50 n_s=50 $\Delta\phi$=9^o	n_c=60 n_s=40 $\Delta\phi$=9^o	n_c=30 n_s=70 $\Delta\phi$=20^o

(a)

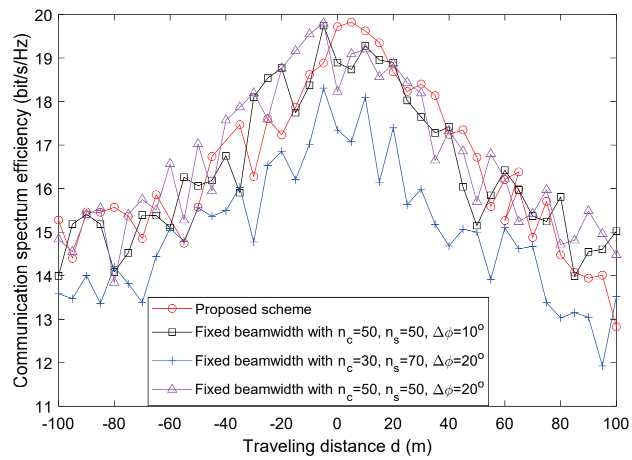

(b)

Fig. 4. (a) Selected actions, (b) the communication spectrum efficiency comparisons.

Fig. 5 depicts the received SINR of sensing echo signals under different schemes. Comparing the two schemes with fixed inter-beam spacing of 20^o and 10^o and 50 antennas respectively allocated for sensing and communication beams, when $d < 0$, at the same position, the larger the inter-beam spacing, the shorter the propagation distance of sensing signals, leading to higher received SINR of echo signals, while it is opposite for $d > 0$. Moreover, at the areas with $d > 0$, sensing distances become larger than communication distances, and therefore the inter-beam interference significantly degrades the sensing SINR of the fixed inter-beam spacing and beamwidth schemes. Although giving more antennas to sensing beams improves the sensing performance to some degree, the received SINR of the scheme with 30 antennas for communications and 70 antennas for sensing is still lower than $SINR_{s,th}$ at the areas (40,100)m. In the proposed scheme, owing to the adaptive adjustments of inter-beam spacing and beamwidth according to dynamic wireless environments, in most areas the received SINR of sensing beams can be maintained higher than the basic requirement $SINR_{s,th}$, except two points near $d = 75m$. Compared with other schemes, the proposed scheme does not always achieve the highest SINR, such as in the area of (-100, 25)m. This is because the sensing optimization object of our proposed scheme is to minimize the sensing spacing distance, so that we can obtain the track inspection data with trains passing through. From the selected actions shown in Fig. 4(a), the proposed scheme can keep smaller inter-beam spacing as well as smaller sensing spacing distance than other schemes. In practice, based on the detection probability and false alarm probability requirements, the SINR threshold of a radar system can be determined, and then we only need to guarantee the received SINR higher than the threshold, from the perspective of which, the proposed scheme achieves the best performance.

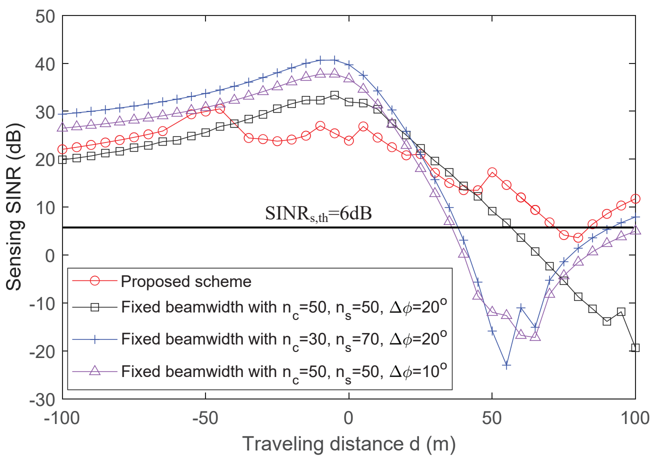

Fig. 5. The received SINR of sensing echo signals.

V. Conclusions and Prospects

In this paper, to improve the communication capacity, and meanwhile to enhance the HSR maintenance efficiency, the joint sensing and communication HSR mmWave wireless network architecture is introduced, where two mmWave beams are intelligently controlled to simultaneously provide broadband mmWave communications and environment sensing. Then, under this network, we analyze the inter-beam interference between sensing and communication beams, and propose the DRL based beam management scheme to balance the communication and sensing performance. Simulation results have demonstrated the effectiveness of our proposed scheme. In our future study, under this joint sensing and communication HSR mmWave wireless network, we will further investigate the beam management during handovers, realizing seamless communications while simultaneously guaranteeing the sensing requirements.

VI. Acknowledgement

The work was supported in part by NSFC under Grant 62101460, 62001071,and 62071393, NSFC High-Speed Rail Joint Foundation under Grant U1834210, Fundamental Research Funds for the Central Universities under Grant 2682020CX78, Project of China Railway Corporation under Grant P2020G004.

References

[1] B. Ai, A. F. Molisch, M. Rupp, and Z.-D. Zhong, “5G key technologies for smart railways,” *Proceedings of the IEEE*, vol. 108, no. 6, pp. 856–893, 2020.

[2] K. Nakamura, N. Iwasawa, K. Kawasaki, N. Shibagaki, Y. Sato, and K. Kashima, “Study of the new application using the millimeter-wave in the railway,” in *2017 IEEE Conference on Antenna Measurements Applications (CAMA), Tsukuba, Japan*, 2017, pp. 20–23.

[3] Z. Feng, Z. Fang, Z. Wei, X. Chen, Z. Quan, and D. Ji, “Joint radar and communication: A survey,” *China Communications*, vol. 17, no. 1, pp. 1–27, 2020.

[4] L. Yan, X. Fang, L. Hao, and Y. Fang, “A fast beam alignment scheme for dual-band HSR wireless networks,” *IEEE Transactions on Vehicular Technology*, vol. 69, no. 4, pp. 3968–3979, 2020.

[5] L. Yan, X. Fang, X. Wang, and B. Ai, “AI-enabled sub-6GHz and mm-Wave hybrid communications: Considerations for use with future HSR wireless systems,” *IEEE Vehicular Technology Magazine*, vol. 15, no. 3, pp. 59–67, 2020.

[6] L. Yan, X. Fang, H. Li, and C. Li, “An mmWave wireless communication and radar detection integrated network for railways,” in *2016 IEEE 83rd Vehicular Technology Conference (VTC Spring), Nanjing, China*, 2016, pp. 1–5.

[7] Q. Xue, P. Zhou, X. Fang, and M. Xiao, “Performance analysis of interference and eavesdropping immunity in narrow beam mmWave networks,” *IEEE Access*, vol. 6, pp. 67 611–67 624, 2018.

[8] F. Liu, C. Masouros, A. Li, H. Sun, and L. Hanzo, “MU-MIMO communications with MIMO radar: From co-existence to joint transmission,” *IEEE Transactions on Wireless Communications*, vol. 17, no. 4, pp. 2755–2770, 2018.

[9] J. Zhao, J. Liu, Y. Nie, and S. Ni, “Location-assisted beam alignment for train-to-train communication in urban rail transit system,” *IEEE Access*, vol. 7, pp. 80 133–80 145, 2019.

[10] M. Gao, B. Ai, Y. Niu, Z. Zhong, Y. Liu, G. Ma, Z. Zhang, and D. Li, “Dynamic mmWave beam tracking for high speed railway communications,” in *2018 IEEE Wireless Communications and Networking Conference Workshops (WCNCW), Barcelona, Spain*, 2018, pp. 278–283.

[11] J. Zhou, T.-H. Chuang, T. Dinc, and H. Krishnaswamy, “Integrated wideband self-interference cancellation in the RF domain for FDD and full-duplex wireless,” *IEEE Journal of Solid-State Circuits*, vol. 50, no. 12, pp. 3015–3031, 2015.

[12] V. Vakilian, J. F. Frigon, and S. Roy, “Effects of angle-of-arrival estimation errors, angular spread and antenna beamwidth on the performance of reconfigurable SISO systems,” in *Proceedings of* IEEE Pacific Rim Conference on Communications, Computers and Signal Processing, Victoria, BC, Canada, Aug. 2011, pp. 515–519.

[13] W. Lu, Antenna theory and technology . Xidian University Press, 2004.

[14] M. Skolnik, Introduction to radar systems. Mcgraw Hill Electrical Engineering, 2001.

[15] M. Volodymyr, K. Koray, S. David, A. A. Rusu, V. Joel, M. G. Bellemare, G. Alex, R. Martin, A. K. Fidjeland, and O. Georg, “Human-level control through deep reinforcement learning,” *Nature*, vol. 518, no. 7540, pp. 529–541, 2019.